



**HAL**  
open science

# Observer-bias and sampling uncertainties in riverine wood flux and volume estimation from video monitoring technique

Hossein Ghaffarian, Bruce Macvicar, Borbala Hortobagyi, Zhi Zhang, Florian Robert, Lise Vaudor, Stéphane Petit, Hervé Piégay

## ► To cite this version:

Hossein Ghaffarian, Bruce Macvicar, Borbala Hortobagyi, Zhi Zhang, Florian Robert, et al.. Observer-bias and sampling uncertainties in riverine wood flux and volume estimation from video monitoring technique. *Earth Surface Processes and Landforms*, 2023, 10.1002/esp.5500 . hal-03848655

**HAL Id: hal-03848655**

**<https://hal.science/hal-03848655>**

Submitted on 22 Feb 2024





**HAL** is a multi-disciplinary open access archive for the deposit and dissemination of scientific research documents, whether they are published or not. The documents may come from teaching and research institutions in France or abroad, or from public or private research centers.

L'archive ouverte pluridisciplinaire **HAL**, est destinée au dépôt et à la diffusion de documents scientifiques de niveau recherche, publiés ou non, émanant des établissements d'enseignement et de recherche français ou étrangers, des laboratoires publics ou privés.



Distributed under a Creative Commons Attribution 4.0 International License

# Observer-bias and sampling uncertainties in riverine wood flux and volume estimation from video monitoring technique

Hossein Ghaffarian<sup>1</sup>  | Bruce MacVicar<sup>2</sup>  | Borbala Hortobagyi<sup>1,3</sup>  |  
Zhi Zhang<sup>1</sup> | Florian Robert<sup>3</sup> | Lise Vaudor<sup>1</sup> | Stéphane Petit<sup>3</sup> | Hervé Piégay<sup>1</sup> 

<sup>1</sup>Environnement-Ville-Société CNRS, Université de Lyon, UMR 5600, Lyon, France

<sup>2</sup>Department of Civil and Environmental Engineering, University of Waterloo, Waterloo, Ontario, Canada

<sup>3</sup>Veodis3D, France

## Correspondence

Hossein Ghaffarian, Université de Lyon, UMR 5600, Environnement-Ville-Société CNRS, F-69362 Lyon, France.

Email: [hossein.ghaffarian@ens-lyon.fr](mailto:hossein.ghaffarian@ens-lyon.fr)

## Funding information

EUR H2O'Lyon, Grant/Award Number: ANR-17-EURE-0018

## Abstract

Wood is an integral part of rivers that can have both positive and negative impacts on natural systems and infrastructures. Different techniques have been developed to quantify wood flux or discharge in rivers. Among them, the stream-side video monitoring technique has proven effective for at-a-station wood monitoring with a high temporal and spatial resolution over an indefinite time period. However, the visual annotation of wood pieces in the videos is subject to uncertainties due to observer bias or 'vision limitations', and video sampling or 'time limitations'. Vision limitations mean that there are patches in the recorded image that may or may not be considered as wood pieces depending on the judgement of the observer. Time limitations mean that the video record may be sampled to estimate the wood flux rather than completing a census of the full record due to the time-consuming nature of continuous visual annotation. To assess these uncertainties, six flood events and 13 video segments corresponding to more than 37 days and 64,000 pieces of wood were analysed on two different rivers (Ain and Allier Rivers in France). The results show that while there is a significant difference between observers for the detection of small wood pieces (< 1 m in length), no significant difference exists for the detection of large wood pieces (> 1 m in length). The application of a truncation length (i.e., considering only wood pieces with a size higher than a certain threshold) reduces the piece number uncertainty significantly without resulting in a meaningful change in the total volume of wood. For the time limitation, it is shown that sampling uncertainty depends on wood flux related to water discharge and flood stages (rising versus falling), so a dynamic sampling strategy that depends on flood stage is recommended.

## KEYWORDS

Ain River, Allier River, uncertainty in wood flux estimate, video monitoring, video sampling, computer vision, drift wood, large wood, observer bias

## 1 | INTRODUCTION

Driftwood is a significant component of riverine corridors both ecologically and morphologically (Abbe & Montgomery, 2003; Battin et al., 2008; Bocchiola, 2011; Gonor et al., 1988; Gregory et al., 2003; Gurnell, 2012; Montgomery et al., 2003; Welber, 2013; Wilcox & Wohl, 2006; Wohl, 2013; Wohl & Scott, 2017). Along with many positive effects, however, wood might be considered as

a risk factor in terms of flooding and infrastructure damage (De Cicco et al., 2018; Lassetre & Kondolf, 2012; Mazzorana et al., 2018; Ruiz-Villanueva et al., 2013; Schmockler & Hager, 2011). Consequently, many attempts have been made to quantify the amount of wood in a river and its transport with laboratory experiments (Lyn et al., 2003; Bocchiola et al., 2008; Ghaffarian et al., 2020), numerical models (Persi et al., 2018, 2019; Ruiz-Villanueva et al., 2014; Yin et al., 2003) and through field

This is an open access article under the terms of the [Creative Commons Attribution-NonCommercial](https://creativecommons.org/licenses/by-nc/4.0/) License, which permits use, distribution and reproduction in any medium, provided the original work is properly cited and is not used for commercial purposes.

© 2022 The Authors. *Earth Surface Processes and Landforms* published by John Wiley & Sons Ltd.

surveys (Gurnell et al., 2002; Piégay et al., 2005; Piégay et al., 2019; Ruiz-Villanueva et al., 2016a; Wohl et al., 2005).

The dynamics of wood in the riverine environment can be studied at different temporal and spatial scales using different monitoring techniques such as plastic tags (Lenzi, 2004; Warren & Kraft, 2008), passive or active radio frequency identifiers (RFID) (MacVicar et al., 2009) or global positioning system (GPS) devices (Ravazzolo et al., 2013). Thanks to rapidly developing new platforms such as kites, microlights, drones, and satellites (Carbonneau & Piégay, 2012; Lejot et al., 2007; Sendrowski & Wohl, 2021), airborne and spaceborne multispectral and hyperspectral imaging systems (Leckie et al., 2005; Marcus et al., 2003, 2002, 2011) and terrestrial or aerial light detection and ranging (LiDAR) (Fleece, 2002; Boivin & Buffin-Bélanger, 2010; Delai et al., 2014; Welling et al., 2021), remote sensing is also widely used to monitor the amount of wood along rivers.

Among various remote sensing studies on wood mobility, ground videography is a technique that can be used to quantify wood transport as a flux (number of pieces) or a discharge (cubic metre per second or hour). Ground videography provides high temporal-resolution data, which is useful for computing rates of transport and fine-scale relationships between wood and water discharges, using a camera that is located in a safe position from flooding on a riverbank or an infrastructure (Benacchio et al., 2017; Kramer & Wohl, 2014; Lyn et al., 2003; MacVicar et al., 2009; MacVicar & Piégay, 2012; Muste et al., 2008). During recent years, there have been many advances in this technique such as measuring the volume of wood only by counting the number of pieces passing through the camera section (Ghaffarian et al., 2020; Zhang et al., 2021), estimating length distribution and transverse distribution of wood pieces (Ghaffarian et al., 2020), and showing the effect of flow discharge on wood recruitment in a river during a flood (MacVicar & Piégay, 2012; Ruiz-Villanueva et al., 2016b; Turowski et al., 2013; Zhang et al., 2021). The original model was based on a limited set of floods from the Ain River that were sufficient to demonstrate a few features such as a threshold of motion ( $\sim 0.6$  of the bankfull discharge,  $Q_{bf}$ ) on this river, high flux during the rising limb of the flood hydrograph, maximum wood flux at  $\sim Q_{bf}$ , and low flux during the falling limb (MacVicar & Piégay, 2012). The extraction of such quantitative information necessitated manual labelling or annotation of the videos. Such a procedure is time-consuming, however, and observers have typically sampled only a portion of the recorded video (MacVicar & Piégay, 2012; Senter et al., 2017), although a few have annotated entire flood events (Boivin et al., 2017; Ghaffarian, Lopez, et al., 2020; Zhang et al., 2021). Advances over the last decade mean that automatic monitoring and detection of wood is now possible (Ali et al., 2012, 2014; Ali & Tougne, 2009; Benacchio et al., 2017; Ghaffarian et al., 2021; Lemaire et al., 2014), as is continuous modeling from flow hydrographs to account for wood flux during conditions with poor visibility such as the nighttime (Zhang et al., 2021). These advances make the technique cheap and efficient, both for scientists as well as urban and river managers.

Despite the clear advantages of an automatic technique, a number of uncertainties remain in the processes of detecting floating wood from streamside videos and building models from flow hydrographs. Ghaffarian et al. (2021), for example, found it necessary to use manual annotations on sample videos to train the software and achieve reliable results. Models of the error associated with different image properties were created to estimate the wood likely missed by

the automatic algorithm. These steps require users to visually detect and measure floating wood, which means that limits in the spatial and temporal resolution of the recorded image and issues related to the visibility of the water surface such as reflectance need to be accounted for. Different users may identify wood differently, which introduces subjectivity into the training data due to user bias. The modeling procedure also relies on manual annotation of video segments to better assess wood variability as a function of the flow hydrograph (Zhang et al., 2021). However, both manual or automatic wood detection procedures are subject to connection or recording limitations for remote cameras, which may also reduce the representativity of the recorded videos because they represent a subset of the videos rather than the entire flood duration.

This study aims to estimate the observer-bias and time-sampling uncertainties in the video monitoring technique. We first address successively the observer-bias and sampling uncertainties and then propose some ways to minimize these uncertainties based on the project requirements. To understand observer-bias, we quantify the variability of manual annotations of different observers on a set of 15-min video segments. For the time-sampling uncertainty we took advantage of a large database of continuously sampled flood events and calculated the variability in wood flux estimates that results from sampling only a portion of these events.

## 2 | STUDY SITES

The data were collected from two different sites, both in France: (i) the Ain River (Figure 1) with 1.5-year flow discharge,  $Q_{1.5} = 840 \text{ m}^3/\text{s}$ , and (ii) the Allier River (Figure 2) with  $Q_{1.5} = 460 \text{ m}^3/\text{s}$ . The Ain River has been the subject of a series of studies on wood flux (piece number per a time interval) and so is relatively well-understood, while there are few if any studies available on the Allier River to this point. The flow discharge is calculated based on the water elevation measured at the gauging station. These data are available online from 1959 on the Ain River and 1986 on the Allier River at ([www.hydro.eaufrance.fr](http://www.hydro.eaufrance.fr)).

The study site in the Ain River is located on its lower reach, a sixth-order piedmont river flowing through a forested corridor in France. The channel is typically single thread with occasional islands, and a freely meandering system with prominent meander scrolls and cutoff channels (Figure 1a) (MacVicar et al., 2009). The longitudinal slope at the study site is 0.17%. The hydrograph shows a strong seasonal pattern, with low flows in the summer and most of the floods occurring between October and April. Bed material sizes are gravel-cobble mix with a median size of 2.5 cm. The unvegetated channel width is 65 m on average at the study site, actively shifting so that a significant amount of wood is delivered by bank erosion. Along the study site, the wood influx has been estimated over several decades from the analysis of aerial photographs at 18 to 38  $\text{m}^3/\text{km}/\text{yr}$  (Lassetre et al., 2008). Floating wood was monitored since 2007 on the river at Pont de Chazey, where a stream gauge is maintained by a regional authority (Figure 1b).

The second study site is located in the lower Allier River, France, in the National Natural Reserve of the Val d'Allier. From its source (1485 m) to its confluence with the Loire (Becc'Allier, 167 m), the Allier River is 410 km long and drains a catchment of 14,400  $\text{km}^2$ . At the study site, the catchment area is 12,980  $\text{km}^2$  and the mean annual

**FIGURE 1** Study site at Pont de Chazey: (a) location of the Ain River course in France and location of the gauging station; (b) camera position and its view angle in yellow [Color figure can be viewed at [wileyonlinelibrary.com](http://wileyonlinelibrary.com)]

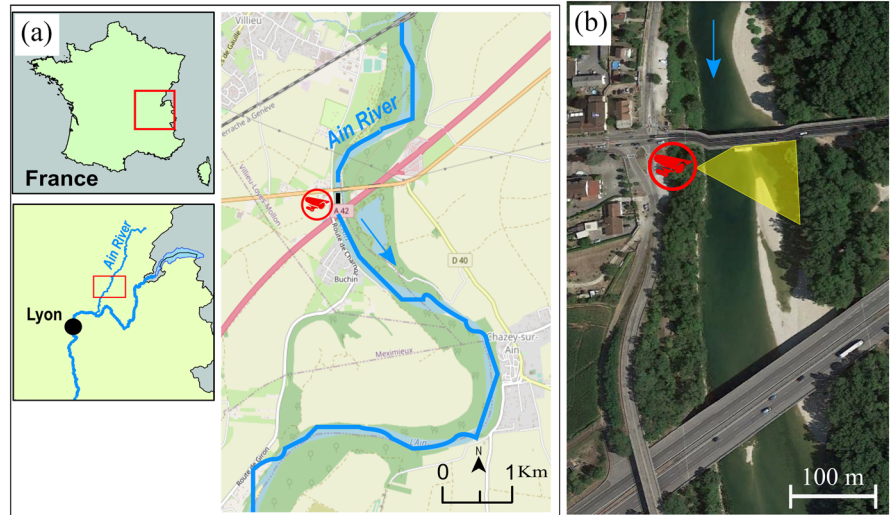
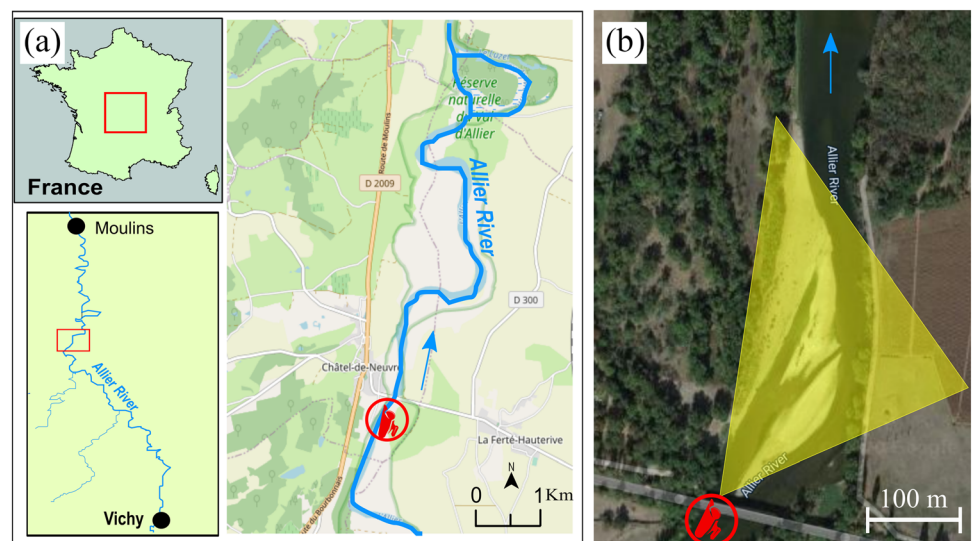


**FIGURE 2** Study site at Châtel-de-Neuvre: (a) location of the Allier River course in France; (b) camera position and its view angle in yellow. [Color figure can be viewed at [wileyonlinelibrary.com](http://wileyonlinelibrary.com)]



flow and biennial flood are respectively 141 and 720 m<sup>3</sup>/s (based on data from the Moulins-sur-Allier gauging station 1968–2005) (Petit, 2006). In this reach, the gravel bed meandering river experienced moderate anthropogenic impact and is characterized by active lateral erosion up to tens of metres per year (Petit, 2006). The hydrological flow regime is pluvio-nival with peak discharge in winter and low flows in summer. The longitudinal slope at the study site is 0.21%. The average active channel width is around 140 m (varies from 100 to 176 m) with a heterogeneous spatial distribution of vegetation patches with different sizes and ages (Breedveld et al., 2006). Since November 2019, floating wood was monitored on the river using a video camera installed at the bridge of Châtel-de-Neuvre, where a stream gauge is maintained by a regional authority (Figure 2b).

Tree species established on both sites are a mix of soft and hardwood species dominated by black poplar (*Populus nigra*) usually with other Salicaceae such as *Salix* sp. (*Salix purpurea*, *Salix triandra*, *Salix viminalis*, *Salix alba*) and on older stages with *Fraxinus excelsior* and *Quercus robur* (Herbst & Dejaifve, 2004). White willow (*S. alba*) forests are rarer but are observed in alluviated former channels (3% of the studied area). *Prunus-Crataegus* shrubs (11% of the studied area) occupied intermediate stages between grassland and hardwood forest (6% of the studied area) (Garófano-Gómez et al., 2017). The reach is a

very diverse landscape mosaic with complex vegetation patches of different sizes and ages (Baptist et al., 2006; Breedveld et al., 2006).

### 3 | MATERIALS AND METHODS

#### 3.1 | Stream-side video camera

On the Ain River, wood pieces were identified and counted using an AXIS P221 Day/Night™ fixed network camera. The camera was located on the side of the river closest to the thalweg to provide a maximum resolution where the majority of wood pieces are observed. The camera elevation is 9.84 m above the base flow surface at a sufficiently wide-angle to afford a view of the entire river width during most periods. Ethernet connectivity enables the automatic transfer of recorded videos to a central server located at University of Lyon, France. Videos were recorded continuously at a frequency of 3 ~ 5 fps and 640 × 480 pixels (for 15-min video segments) and 768 × 576 pixels (for continuous flood events). On the Allier River, wood pieces were monitored using a Hikvision DS-2CD2T42WD-I8 6 mm fixed network camera. Videos were recorded continuously at a frequency of 6 fps and a resolution of 1920 × 1080 pixels. The Allier camera is positioned close to the

thalweg at 11 m above the baseflow surface, similar to the Ain River, but it is installed on a bridge and faces downstream. Pixel sizes from the two points of view vary from ~1 cm to ~1 m.

Using a manual algorithm, written in Matlab R2017a, video playback was initiated and stopped by the user when a piece of wood was observed following the procedure described in MacVicar and Piégay (2012). Both ends of wood pieces were then digitally annotated on the stopped video frame and the video was advanced to a later frame where the ends of the wood pieces were again digitally annotated. Video frames were rectified and pixel locations calculated in cartesian coordinates (Ghaffarian, Piégay, et al., 2020). The length of each wood piece ( $L$ , in metres) was then calculated. The volume of each piece of wood ( $V$ , in  $m^3$ ) was calculated as a function of  $L$  following the approach proposed by Ghaffarian, Lopez, et al. (2020) on the Ain River, with the difference that Ghaffarian, Piégay, et al. (2020) calculated volume from the measured object length and an empirical relation between length and diameter while here we calculate volume ( $V$ ) directly based on an empirical relation with the object length ( $L$ ) as  $V(L) = 0.0077L^{2.3}$ . The validity of using the same function for both rivers is discussed in Section 5.2.

### 3.2 | Studied events

According to the main purposes of this study, two different strategies were applied: (i) monitoring 15 min video segments and (ii) monitoring

continuous flood events. As shown in Table 1, five different observers monitored and detected 11 video segments on the Ain River and four observers monitored and detected two video segments on the Allier River in order to assess observer bias. The 15 min video segments were selected such that they corresponded with different light conditions (e.g., sunshine or cloudy weather or different day times), in order to evaluate observer-bias in a wide range of contexts. Videos were also selected so that the amount of wood pieces varied greatly (from 0 to more than 300) to evaluate whether observer-bias is affected by the absolute flux. For the second objective to assess the effect of sampling strategies on estimations and uncertainties, six flood events from both the Ain and Allier Rivers were continuously monitored by a single observer. In total, around 37 days of video with more than 64,000 detected pieces was annotated for this second objective (Table 2).

### 3.3 | The reliability of observers and the observer bias

In this study, the annotations were acquired by four to five different observers. The observers had no experience when they did their annotations on these videos, and these videos were used to train them and see if their decision in scoring wood was similar to others. The difference between observers was first tested by checking the overall distribution of wood piece lengths and lateral position on both

**TABLE 1** Sampled 15 min video segments

River	Date	Time	Number of wood pieces detected by observers					Wood flux (piece/min)	
			Observer 1	Observer 2	Observer 3	Observer 4	Observer 5	Mean	Standard deviation
Ain	22 November 2007	9:15 AM	0	0	0	0	0	0.0	0.0
	22 November 2007	11:15 AM	0	0	0	0	0	0.0	0.0
	22 November 2007	12:00 AM	1	0	1	0	1	0.0	0.0
	22 November 2007	3:56 PM	11	12	12	10	8	0.7	0.1
	22 November 2007	5:11 PM	4	4	5	5	3	0.3	0.1
	23 November 2007	7:56 AM	313	226	293	275	313	18.9	2.4
	23 November 2007	9:56 AM	354	313	386	358	326	23.2	1.9
	23 November 2007	10:11 AM	290	216	236	225	210	15.7	2.1
	23 November 2007	11:56 AM	337	175	243	253	183	15.9	4.4
	23 November 2007	2:26 PM	253	95	143	118	92	9.3	4.4
23 November 2007	5:05 PM	271	136	216	179	130	12.4	3.9	
Allier	25 November 2019	3:33 PM	672	–	643	366	408	34.8	10.5
	23 December 2019	11:15 AM	191	–	92	108	128	8.7	2.9

**TABLE 2** Continuous monitoring statistics

River	Flood periods	$Q_{max}$ ( $m^3/s$ )	Analysed video (hr)	Total amount of wood	
				Number	Volume ( $m^3$ )
Ain	15–16 December 2012	932	17:15	7,697	504
	1–6 February 2013	701	56:30	1,465	105
	21–24 January 2018	1430	25:45	8,871	310
Allier	23–28 November 2019	494	70:00	24,587	1,109
	15–16 December 2019	348	20:00	3,453	129
	21–30 December 2019	530	100:00	12,773	346

ivers. Both distributions should be unique in a cross-section (Ghaffarian, Lopez, et al., 2020) but relatively consistent between observers.

To further study the observer-bias, we then calculated the total piece number and the total wood volume for each observer, and then applied a truncation length such that pieces with length less than this truncation length were removed from the database of each observer. We expect that observer-bias is relevant for coarse particulate organic matter (CPOM) (Turowski et al., 2013) (< 1 m) where it is difficult to decide if something observed in the video is wood or not. This uncertainty is thought to be higher where pieces are partially emerged from the water, pixels around the piece are blurry, or there is a lack of contrast between wood and water pixel colours, so that size is a critical parameter. Truncation is a way to minimize the observer bias and we expect removing smaller pieces should not have effects on overall wood volume estimate.

### 3.4 | Sampling time window

To study the effect of the sampling time window on the accuracy of data acquisition, a flood event duration was divided into equal time intervals, each with duration  $\Delta t$  (in this study  $\Delta t = 60$  min (Figure 3)). A sample time  $dt$  was selected and the ratio of sampled time to total time defined as the time window. The total amount of wood was then calculated by extrapolating the annotated data inside  $dt$  using the ratio of  $\Delta t/dt$ . Sub-sampling the data in this fashion means that the 'total detection' will be different from the total amount of wood in river estimated by a complete annotation of wood due to the non-uniform distribution of wood within  $\Delta t$ . To calculate the variability associated with this sub-sampling, we also varied the starting time of  $dt$  from  $t_0 = 0$  to  $t_0 = \Delta t - dt$ .

Because the average magnitude of wood flux varies according to flow conditions and flood stages, it is expected that these variables

will also strongly affect the variability of wood flux measurements. We therefore considered a dynamic sampling strategy by classifying flow discharge into four groups on each of the rising and falling limbs (i.e.,  $0 < Q/Q_{1.5} \leq 0.5$ ,  $0.5 < Q/Q_{1.5} \leq 1$ ,  $1 < Q/Q_{1.5} \leq 1.5$ , and  $1.5 < Q/Q_{1.5} \leq 2$ ), for a total of eight groups. The variability was then assessed for each group as the difference between detected and total number normalized by the total number of wood pieces ( $|N_{total} - N_{detected}|/N_{total}$ ), and the same for volume, for different time windows from 1 min to 60 min (see later in Figure 8). The uncertainty index was then introduced for each of these eight groups as the integral of the uncertainty values for different time windows (from 1 min to 60 min). These uncertainty indexes make uncertainty on both rivers comparable. We also used these indexes to show which part of hydrograph is the most important part to monitor (see later in Figure 9). And finally, thanks to these indexes we introduce three major groups for an optimum sampling strategy (see later in Figure 11).

## 4 | RESULTS

### 4.1 | Wood length distribution and transverse position

The length distribution and transverse position of wood pieces were compared among observer annotations to check their reliability. No ground truth value was available, so the median value of all observers was used for comparison (the red line in boxplots in Figure 4). As shown on Figure 4(a, b), the wood length distribution is similar among different observers and in both rivers. Also similar for both rivers are that most of the wood pieces were annotated in a 10% of the river section (Figure 4c, d), though the lateral position is different for the two rivers as wood was detected from 15 to 25% of the width on the Ain and from 5 to 15% on the Allier. These similarities confirm that the data provided by all observers are reliable. The fact that length

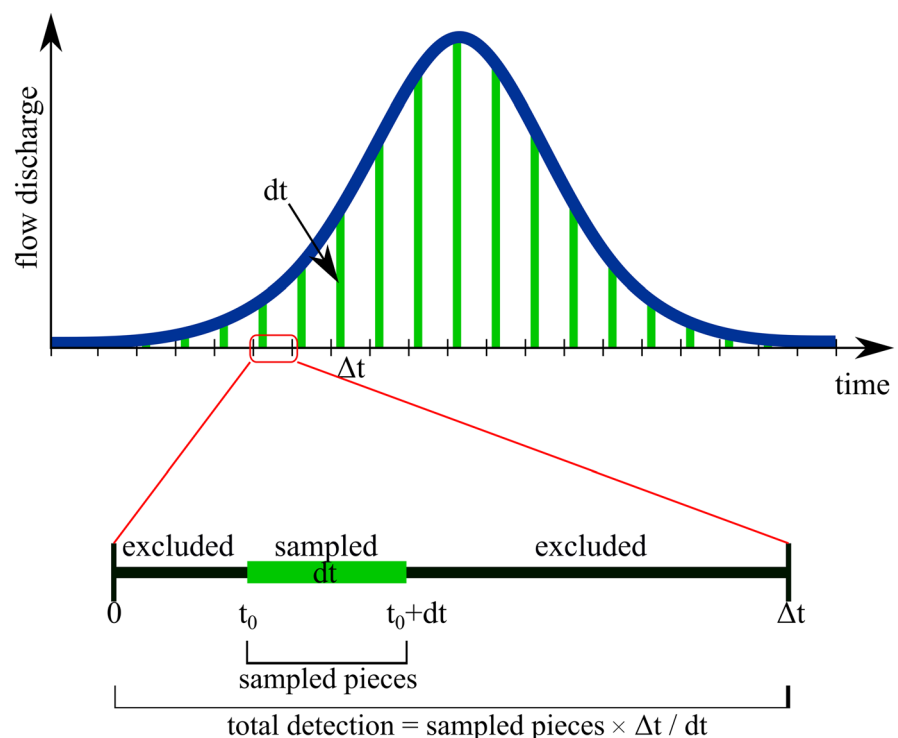


**FIGURE 3** Schematic view of the sampling time window [Color figure can be viewed at [wileyonlinelibrary.com](http://wileyonlinelibrary.com)]

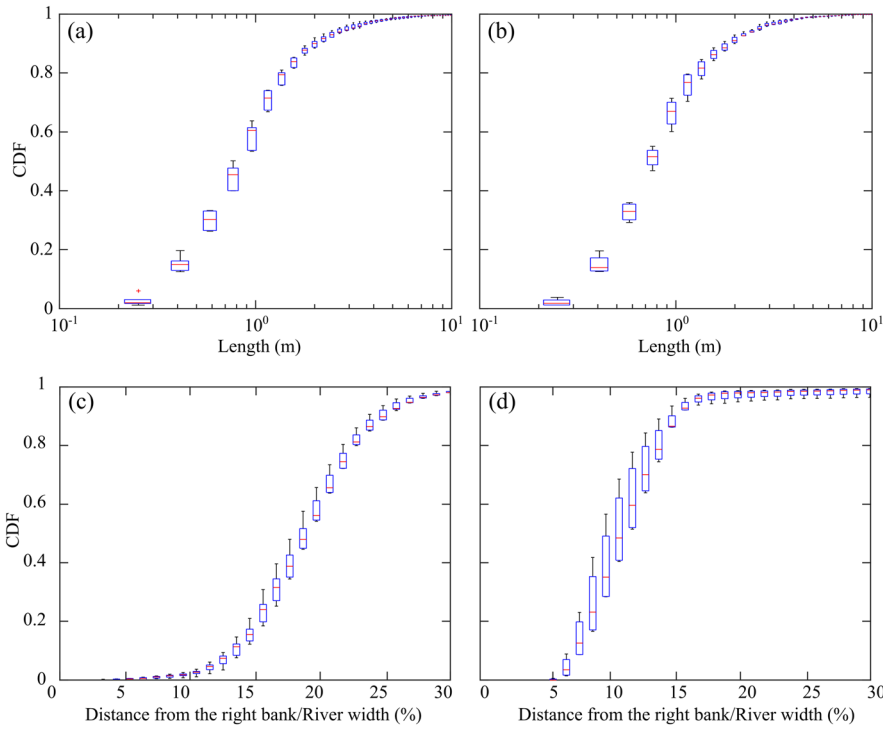


**FIGURE 4** Comparison of the results of different observers for cumulative distribution function (CDF) of (a, b) wood length and (c, d) transversal position of wood pieces, on the Ain River (a, c), and Allier River (b, d). [Color figure can be viewed at [wileyonlinelibrary.com](http://wileyonlinelibrary.com)]

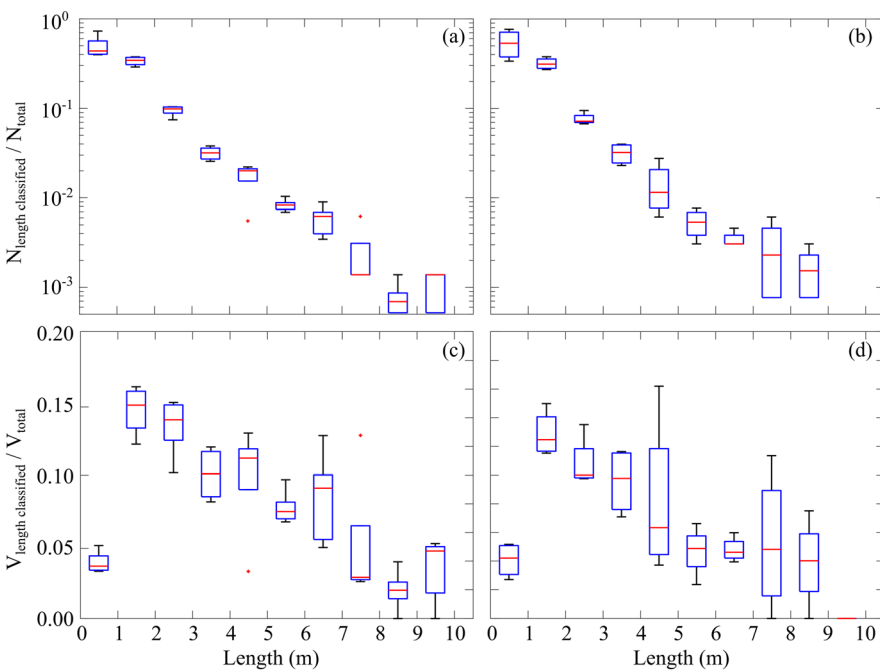


**FIGURE 5** Classification of results based on piece length; (a, b) normalized piece number and (c, d) normalized piece volume on the Ain River (a, c) and Allier River (b, d) with five and four samples, respectively. On each box, the central mark indicates the median, and the bottom and top edges of the box indicate the 25th and 75th percentiles, respectively. The whiskers extend to the most extreme data points not considered outliers. Note that the x-axis was truncated at 10 m to focus on the distribution of the smaller size wood. [Color figure can be viewed at [wileyonlinelibrary.com](http://wileyonlinelibrary.com)]

distribution and wood transverse distribution are in the same range also confirms that using the average value of all observers as the ‘true’ value is a reasonable assumption. Despite the similarities, however, there are important differences between the observers as described in the following section.

## 4.2 | Uncertainty on piece number and volume according to piece lengths

The difference of piece number between different observers was assessed using boxplots grouped by wood length (Figure 5). As shown, the frequency of pieces less than 1 m in length was high in both rivers,

but different observers recorded different frequencies in this size class, which resulted in a high variability of the estimate. For illustration, the largest number of the detected wood pieces were in the CPOM size class, but the relative proportion could be over 40% or less than 70% depending on the river and the observer (Figure 5a, b). The lower bound is subject to observer judgement because of the high frequency of these pieces and their small size such that observers may consider them as insignificant. Despite their high frequency, it is also apparent that they represent only ~4% of the total wood volume even for observers that detect them in large numbers (Figure 5c, d). In contrast, wood pieces longer than 5 m are relatively infrequent, but even single observations of these large pieces can represent a significant portion of the total wood. Their

large size also means that they are rarely missed by observers. However, there is considerable uncertainty in their volume due to the subjectivity of identifying their precise endpoints. In the Allier River in particular the wood pieces are relatively far from the camera, so small variations in the endpoint selection will lead to large variation in volume estimates.

The considerations on the observer variability and impact on piece volume estimates led us to recommend a strategy of a truncation length to minimize observer biases. As shown on Figure 6, progressively higher proportions of wood pieces are removed from the database as the truncation length increases from 0 to 1 m (Figure 6a), but wood volume is relatively insensitive to the truncation length in this range (Figure 6b). A truncation length of 1 m, for example, reduces wood frequency by 50% but reduces wood volume by < 10%. The confidence bounds also show that longer truncation lengths significantly reduce the variability of the wood frequency estimates (Figure 6a) without any apparent change in the uncertainty of the volume (Figure 6b). These patterns again suggest that operators were inconsistent in their detection and recording of the smaller wood sizes but that they can be removed from the database without a significant change in total wood volume. A 1 m in length as suggested by previous authors (Wohl et al., 2010) is then an appropriate threshold at the spatial resolution of the images in this study.

**FIGURE 6** Effect of using a truncation length on (a) normalized piece number and (b) normalized piece volume. Solid line shows the median value and upper and lower dashed lines show first and third quartile of data as the confident bounds. [Color figure can be viewed at [wileyonlinelibrary.com](http://wileyonlinelibrary.com)]

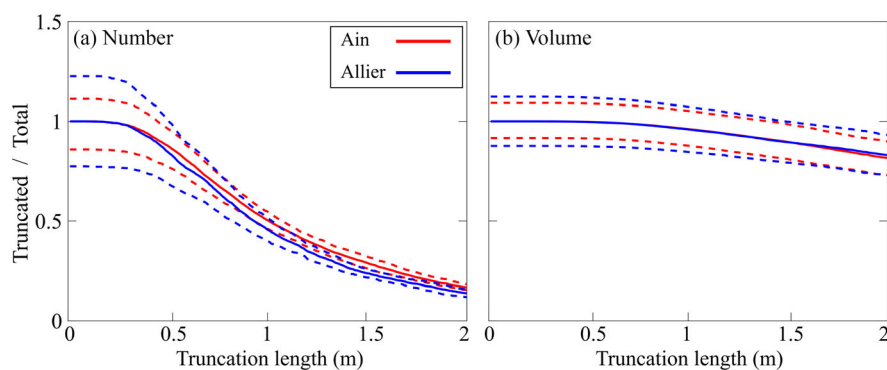
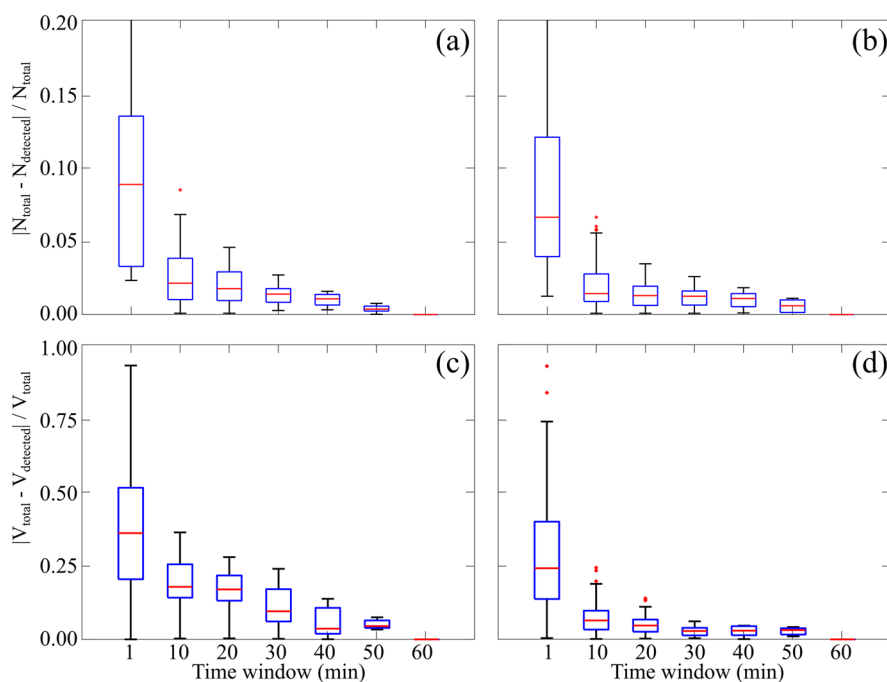


**FIGURE 7** The proportion of detected piece number (a, b) and volume (c, d) due to time excluded from sampling as a function of time window on the Ain River (a, c) and Allier River (b, d). Detected number/volume are calculated from sampling and the total number/volume is what annotated by continuous annotation (see Section 3.4). Note that as 'detected number - total number' is almost symmetric on the positive and negative parts, we used the absolute value here which makes the uncertainty index easier to present in next figures. [Color figure can be viewed at [wileyonlinelibrary.com](http://wileyonlinelibrary.com)]



### 4.3 | Uncertainties associated with sampling time window

Sampling a fraction of videos significantly reduces monitoring costs but increases uncertainties in wood frequency and volume estimate. Following the method described in Section 3.4, a linear relation between the fraction of monitored videos and the fraction of detected wood pieces can be established. However, uncertainty for piece number and volume is relatively high when sampling times are low (Figure 7), and this uncertainty decreases rapidly as the sampling time window is increased.

As described in section 3.4, flow discharge was separated into eight classes on the rising and falling limbs and the uncertainty was calculated for each class. Figure 8 shows an example of the piece number uncertainty on the Ain River for  $1 < Q/Q_{1.5} < 1.5$  during the rising limb of the flood hydrograph. Though not shown here for the sake of brevity, separate boxplots from individual floods plotted in similar ranges but were more variable due to gaps in the data during the night. For this reason, the uncertainty by discharge class was calculated from the average of three floods on each of the Ain and Allier Rivers.

To summarize the results from the discharge class analysis we calculated an uncertainty index, which was defined as the integral of



the 99% confidence bound (as shown in Figure 8). Despite some differences between the two rivers, three stages are apparent for the uncertainty as a function of discharge class (Figure 9): (i) high uncertainty for  $Q/Q_{1.5} > 0.5$  on the rising limb, (ii) smaller uncertainty for the same range but on the falling limb, and (iii) very small uncertainty for  $Q/Q_{1.5} \leq 0.5$ . According to Figure 9 the uncertainty for detecting wood pieces is low when  $Q/Q_{1.5} < 0.5$ , which means that sampling time windows can be relatively small during these lower flow periods. Not a lot of wood passes during these low flow stages and the few wood pieces that pass are not significant for estimating overall wood fluxes. During a flood, however, wood volumes and uncertainty increase markedly. A significant difference is apparent between the rising and falling limbs, with the rising limb presenting a particular challenge due to the peak in the uncertainty that occurs between  $0.5 \leq Q/Q_{1.5} \leq 1.0$ . The uncertainty gradually decreases with flows above  $Q_{1.5}$  and on the falling limb of the flood. A practical example of optimizing the sampling strategy to match uncertainty in these three stages is described in Section 5.3.

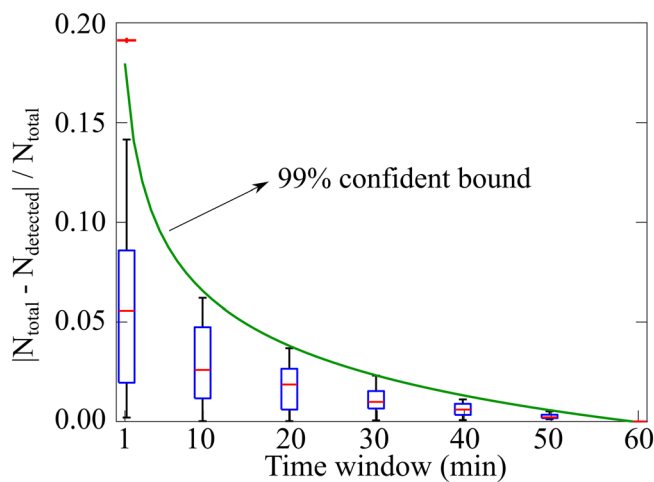


**FIGURE 8** The proportion of detected piece number due to time excluded from sampling as a function of time window on the Ain River and for  $1 < Q/Q_{1.5} < 1.5$  on the rising limb of the flood hydrograph. [Color figure can be viewed at [wileyonlinelibrary.com](https://onlinelibrary.wiley.com)]

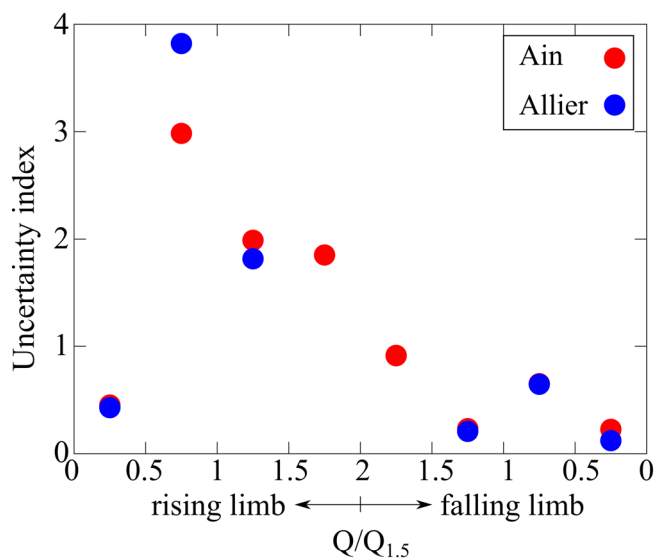


**FIGURE 9** Uncertainty index as a function of flow discharge [Color figure can be viewed at [wileyonlinelibrary.com](https://onlinelibrary.wiley.com)]

## 5 | DISCUSSION

### 5.1 | Observer bias in frequency and volume estimate

Piece number and volume are the two main factors to quantify wood transport through a river section. While the first is the most readily available measure in video monitoring, the second also depends on the size of floating pieces, which is related to image resolution as well as the piece diameter with some additional uncertainty in the estimated volume due to observer bias (observers may select different pixels as the borders of a wood piece) (Ghaffarian et al., 2021). For example, where the pixel size is in the order of 1 cm near the camera, a one-pixel difference between two different observers will result in an uncertainty in the length estimate of the wood piece on the order of 1 cm. However, a similar observer difference for a wood piece far from the camera will introduce an uncertainty on the order of 1 m. In the same way, visual differences created by field conditions such as waves or sun reflection on the river surface can result in differences between observers when selecting the pixels to define the wood piece geometry or even whether an object is identified as a piece of wood or not. The video from the Ain River taken on 23 November 2007 at 2:26 PM (see Table 1) is a good example showing a big difference of piece number between different observers. In this video, the windy weather and relatively low light due to overcast conditions reduced the ease with which wood objects could be detected from the images.

Based on our observations on two different rivers, the reliability of video monitoring directly relates to the size of wood pieces. In the case of CPOM ( $< 1$  m), there is more than 70% uncertainty on piece number among different observers (Figure 5a). In contrast, observer annotation is quite reliable for detecting large wood pieces. Therefore, by applying a truncation length, the uncertainty on piece number drops down without any considerable change in total volume (e.g., from more than 20% when  $L_{tr} = 0$  to less than 5% for  $L_{tr} = 1$  m, while less than 3% change was observed for the total volume of wood). In contrast, the uncertainty on wood volume is more consistent and is thought to be related to optical limitations (resolution, luminosity, etc.) and natural conditions (partial wood submersion, flow roughness) rather than the observer bias, high discharge or exceptional wind and so on, which still needs to be explored (Ghaffarian, Lopez, et al., 2020; MacVicar & Piégay, 2012; Zhang et al., 2021). It should be noted that not only manual annotations are affected by the wood length, but also Ghaffarian, Piégay, et al. (2020) showed the wood length is a crucial parameter in the accuracy of the automatic detection and that wood volume estimates are increasingly sensitive to this parameter as the distance between the wood and the camera increases. In brief, our observations confirm that it is necessary to (i) position the camera in a way that most of the wood pieces are passing close to the camera and (ii) apply a truncation length to the data set to limit the observer bias. There is therefore a need to carefully define the target spatial resolution for inter-river comparisons so that the vision limitation on uncertainty can be properly accounted for. In this study most of the pieces (more than 90%) were detected where the spatial resolution was less than 10 cm (5 cm in average), which we showed is enough to detect wood pieces as small as 1 m without significant operator bias.

Moreover, more resolution (smaller pixel size) will result in increased accuracy when visually assessing the object borders, which should result in less uncertainty on wood length and volume. However, based on our observations, uncertainty on piece number (less than 1 m in length) depends on observer judgement rather than the camera resolution. Even close to the camera with very small pixel size there were always some patches in the video that some observers considered as wood while others did not. For pieces longer than 1 m all observers had a similar judgement.

## 5.2 | Link between piece length and volume

As explained in Section 3.1, we used the same relationship between length and volume on both rivers. The goal here was to adjust this strategy to calculate wood volume. The positive relation between wood length on the accuracy of acquired data was also observed by Ghaffarian, Piégay, et al. (2020). They compared the results of the length distribution in two different conditions: (i) wood pieces passing in front of the camera (on the Ain River) and (ii) wood pieces passing far from the camera (on the Isère River, France). Their comparison reveals that while the length distribution for pieces more than 2 m ( $L_{tr} > 2m$ ) was quite similar, it was totally different for small pieces ( $L_{tr} < 1m$ ). Here, we used the same approach to check the validity of using the same relation between wood length and volume on both rivers. As it is seen in Figure 10 there is a similar wood length distribution on both rivers with the correlation of 99% between two length distribution vectors. Therefore, (i) a similar wood length distribution, (ii) the same dominant species on both sites, and (iii) a good position for the camera (near the transverse position where most of the wood pieces are passing and with almost same pixel size distribution in both sites (Ghaffarian et al., 2021)), supports the use of the same relationship between length and volume on the Allier River. It should be noted that uncertainty in piece number is also observed in channel width as a function of the distance from the camera and image resolution. However, most pieces pass around the same lateral position in both rivers, and there was enough data only in around 20m of the river width which have almost the same resolution.

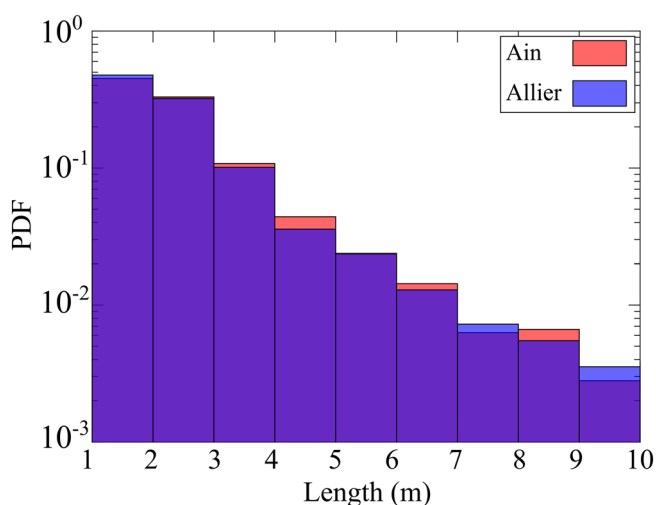


**FIGURE 10** Comparison of the wood length distribution on the two studied rivers. [Color figure can be viewed at [wileyonlinelibrary.com](https://onlinelibrary.wiley.com)]

## 5.3 | Uncertainties associated with sampling videos

Based on our observations, a static sampling strategy (i.e., using a constant time window over the duration of a flood) is sub-optimal due to the sensitivity of the sampling error to flow discharge and flood stage. As a practical recommendation for sampling, we defined three main groups for the discharge classes (described in Section 4.3); as: (i)  $Q/Q_{1.5} > 0.5$  on the rising limb, (ii)  $Q/Q_{1.5} > 0.5$  on the falling limb, and (iii)  $Q/Q_{1.5} \leq 0.5$ . A larger number of groups could be used, but based on our experience in monitoring hundreds of hours of floods and considering the random effects of the river and different shapes of flood hydrograph, these three groups are the most practical. Figure 11 shows the uncertainty of sampling for the three stages of flood based on the three discharge groups. The uncertainty based on a static sampling strategy (a constant time window all along a flood) according to the data presented in Figure 7 is shown for comparison. Note that the presented results average all events from both rivers.

Figure 11 can be used to select an appropriate sampling strategy according to the sensitivity of the study. For example, if the goal is to attain a 5% uncertainty in the annotations, the optimal strategy would be to sample for 20 min every hour on the rising limbs of the floods and to not sample during the rest of the flooding period, which together represents less than 1% of the total wood flux uncertainty. Moreover, the close agreement between the data on the rising limb (red line) and the static sampling (black line) shows that sampling only on the rising limb can reasonably represent the wood mobility in the river, which considerably reduces monitoring effort. Moreover, the effect of the dynamic time window is negligible for discharges less than  $0.5Q_{1.5}$  (green line) which agrees with MacVicar and Piégay (2012). Therefore, a practical recommendation to monitor the maximum amount of wood in an optimum amount of time is to monitor only floods above a certain discharge threshold and to prioritize the rising limb of the flood. However, it should be noted that this method can only be used as a rough guess to limit the uncertainties.

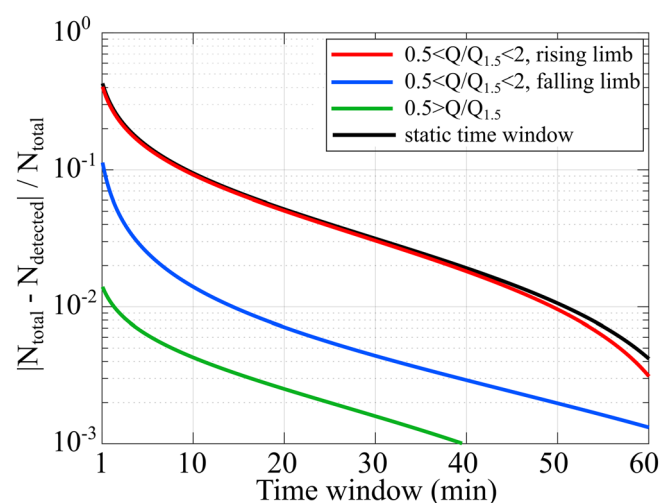


**FIGURE 11** Practical chart for establishing a sampling strategy [Color figure can be viewed at [wileyonlinelibrary.com](https://onlinelibrary.wiley.com)]

## 6 | CONCLUSIONS

In this study we examined two sources of uncertainty that result from applying video monitoring for wood quantification: (i) observer bias or vision limitation, and (ii) video sampling or time limitation. To assess these sources of uncertainty, six flood events and 13 video segments were monitored by four to five observers on two rivers, Ain and Allier, France.

The results show that using a truncation length significantly reduces the number of counted wood pieces, but has little impact on total wood volume. For the video sampling, selecting an appropriate sampling strategy can reduce monitoring time without significantly increasing the uncertainty of wood frequency estimates. For this purpose, it is recommended that a dynamic sampling time that varies with the flow discharge and flood stages be used rather than a constant value. Future studies will be needed to quantify remaining uncertainties related to wood volume estimation and submergence.

Finally, as mentioned, these videos were used to train different observers and see if their decision in scoring wood was similar to others. To do so, we make these videos available as a training set in the Supporting information so that people can assess their scoring experience.

## ACKNOWLEDGEMENTS

The work was performed within the framework of the EUR H2O'Lyon (ANR-17-EURE-0018) of Université de Lyon (UdL) through the 'Investissements d'Avenir' programme operated by the French National Research Agency (ANR) Data availability statement.

The authors thank two external reviewers and Professor Lane for their comments and suggestions that significantly improved the article.

One of the first papers the last author of this contribution read for his master's thesis was written by Ken J. Gregory on 'Coarse Woody Debris' in streams channels. The authors have had the opportunity to meet Ken several times since then, cooperate and interact passionately with him on wood and widely on riverine science. Ken was an inspiring gentleman-scientist and an example for all of us in the domain showing how to practice sciences and behave with others. Until recently he was still discussing advances on 'in-channel wood' with us providing always helpful suggestions and we expect this contribution should have interested him. Thank you, Ken.

## DATA AVAILABILITY STATEMENT

The videos used in this study to estimate operator bias are attached as embedded material for future use by other researchers or operator training.

## ORCID

Hossein Ghaffarian  <https://orcid.org/0000-0002-6854-689X>

Bruce MacVicar  <https://orcid.org/0000-0001-7227-974X>

Borbala Hortobágyi  <https://orcid.org/0000-0002-0105-9456>

Hervé Piégay  <https://orcid.org/0000-0002-3864-2119>

## REFERENCES

Abbe, T.B. & Montgomery, D.R. (2003) Patterns and processes of wood debris accumulation in the Queets river basin, Washington.

*Geomorphology*, 51(1-3), 81–107. Available from: [https://doi.org/10.1016/S0169-555X\(02\)00326-4](https://doi.org/10.1016/S0169-555X(02)00326-4)

Ali, I., Mille, J. & Tougne, L. (2012) Space-time spectral model for object detection in dynamic textured background. *Pattern Recognition Letters*, 33(13), 1710–1716. Available from: <https://doi.org/10.1016/j.patrec.2012.06.011>

Ali, I., Mille, J. & Tougne, L. (2014) Adding a rigid motion model to foreground detection: Application to moving object detection in rivers. *Pattern Analysis and Applications*, 17(3), 567–585. Available from: <https://doi.org/10.1007/s10044-013-0346-6>

Ali, I. & Tougne, L. (2009) Unsupervised Video Analysis for Counting of Wood in River during Floods. In: Bebis, G., et al. (Eds.) *Advances in visual computing*. Berlin, Heidelberg: Springer Berlin Heidelberg, pp. 578–587. [online] Available from: [http://link.springer.com/10.1007/978-3-642-10520-3\\_55](http://link.springer.com/10.1007/978-3-642-10520-3_55) Accessed 2 March 2020.

Baptist, M. J., Haasnoot, M., Cornelissen, P., Icke, J., van der Wedden, G., de Vriend, H. J. & Gugić, G. (2006) Flood detention, nature development and water quality along the Lowland River Sava, Croatia. *Hydrobiologia*, 565, 243–257. <https://doi.org/10.1007/s10750-005-1917-3>

Battin, T.J., Kaplan, L.A., Findlay, S., Hopkinson, C.S., Marti, E., Packman, A. I., Newbold, J.D. & Sabater, F. (2008) Biophysical controls on organic carbon fluxes in fluvial networks. *Nature Geoscience*, 1(2), 95–100. Available from: <https://doi.org/10.1038/ngeo1101>

Benacchio, V., Piégay, H., Buffin-Bélanger, T. & Vaudor, L. (2017) A new methodology for monitoring wood fluxes in rivers using a ground camera: Potential and limits. *Geomorphology*, 279, 44–58. Available from: <https://doi.org/10.1016/j.geomorph.2016.07.019>

Bocchiola, D. (2011) Hydraulic characteristics and habitat suitability in presence of woody debris: A flume experiment. *Advances in Water Resources*, 34(10), 1304–1319. Available from: <https://doi.org/10.1016/j.advwatres.2011.06.011>

Bocchiola, D., Rulli, M.C. & Rosso, R. (2008) A flume experiment on the formation of wood jams in rivers. *Water Resources Research*, 44(2), W02408. Available from: <https://doi.org/10.1029/2006WR005846>

Boivin, M. & Buffin-Bélanger, T. (2010) Using a terrestrial LIDAR for monitoring of large woody debris jams in gravel-bed rivers. 5–10 pp.

Boivin, M., Buffin-Bélanger, T. & Piégay, H. (2017) Interannual kinetics (2010–2013) of large wood in a river corridor exposed to a 50-year flood event and fluvial ice dynamics. *Geomorphology*, 279, 59–73. Available from: <https://doi.org/10.1016/j.geomorph.2016.07.010>

Breedveld, M., Liefhebber, D., Geerling, G.W., Smits, A.J.M., Ragas, A.M.J., Leuven, R. & van den Berg, J.H. (2006) Succession and rejuvenation in floodplains along the river Allier (France). In: *Living Rivers: Trends and challenges in science and management*. Springer, pp. 71–86.

Carbonneau, P. & Piégay, H. (2012) *Fluvial remote sensing for science and management*. Chichester, UK: John Wiley & Sons. Available from: <https://doi.org/10.1002/9781119940791>

De Cicco, P.N., Paris, E., Ruiz-Villanueva, V., Solari, L. & Stoffel, M. (2018) In-channel wood-related hazards at bridges: A review. *River Research and Applications*, 34(7), 617–628. Available from: <https://doi.org/10.1002/rra.3300>

Delai, F., Moretto, J., Picco, L., Rigon, E., Ravazzolo, D. & Lenzi, M.A. (2014) Analysis of morphological processes in a disturbed gravel-Bed River (Piave River): Integration of LiDAR data and colour bathymetry. *Journal of Civil Engineering and Architecture*, 8, 639–648. Available from: <https://doi.org/10.17265/1934-7359/2014.05.014> Available from: <http://www.davidpublisher.org/index.php/Home/Article/index?id=7832.html>

Fleece, W.C. (2002) Modeling the Delivery of Large Wood to Streams with Light Detection and Ranging (LIDAR) Data 1. USDA Forest Service Gen. Tech. Rep. PSW-GTR-181 2: 71–83.

Garófano-Gómez, V., Metz, M., Egger, G., Díaz-Redondo, M., Hortobágyi, B., Geerling, G., Corenblit, D. & Steiger, J. (2017) Vegetation succession processes and fluvial dynamics of a mobile temperate riparian ecosystem: The lower Allier River (France). *Géomorphologie: Relief, Processus, Environnement*, 23(3), 187–202.

Ghaffarian, H., Lemaire, P., Zhi, Z., Tougne, L., MacVicar, B. & Piégay, H. (2021) Automated quantification of floating wood pieces in rivers

- from video monitoring: A new software tool and validation. *Earth Surface Dynamics*, 9(3), 519–537. Available from: <https://doi.org/10.5194/esurf-9-519-2021>
- Ghaffarian, H., Lopez, D., Mignot, E., Piegay, H. & Riviere, N. (2020) Dynamics of floating objects at high particulate Reynolds numbers. *Physical Review Fluids*, 5(5), 054307. Available from: <https://doi.org/10.1103/PHYSREVLUIDS.5.054307>
- Ghaffarian, H., Piégay, H., Lopez, D., Rivière, N., MacVicar, B., Antonio, A. & Mignot, E. (2020) Video-monitoring of wood discharge: First inter-basin comparison and recommendations to install video cameras. *Earth Surface Processes and Landforms*, 45(10), 2219–2234. Available from: <https://doi.org/10.1002/esp.4875>
- Gonor, J.J., Sedell, J.R. & Benner, P.A. (1988) What we know about large trees in estuaries, in the sea, and on coastal beaches. In: Maser, C., Tarrant, R.F., Trappe, J.M. & Franklin, J.F. (Eds.) *From the forest to the sea, a story of fallen trees*. Pacific Northwest Res. Sta., Portland, OR: USDA For. Serv. Gen. Tech. Rep. GTR-PNW-229, pp. 83–112. tech
- Gregory, S., Boyer, K.L. & Gurnell, A.M. (2003) Ecology and management of wood in world rivers, <https://doi.org/10.47886/9781888569568>
- Gurnell, A.M. (2012) Wood and river landscapes. *Nature Geoscience*, 5(2), 93–94. Available from: <https://doi.org/10.1038/ngeo1382>
- Gurnell, A.M., Piégay, H., Swanson, F.J. & Gregory, S.V. (2002) Large wood and fluvial processes. *Freshwater Biology*, 47(4), 601–619. Available from: <https://doi.org/10.1046/j.1365-2427.2002.00916.x>
- Herbst, S. & Dejaifve, P.A. (2004) *La réserve naturelle nationale du val d'Allier*. France: Direction régionale de l'environnement. Auvergne rhone alpes.
- Kramer, N. & Wohl, E. (2014) Estimating fluvial wood discharge using time-lapse photography with varying sampling intervals. *Earth Surface Processes and Landforms*, 39(6), 844–852. Available from: <https://doi.org/10.1002/esp.3540>
- Lassetre, N.S. & Kondolf, G.M. (2012) Large woody debris in urban stream channels: Redefining the problem. *River Research and Applications*, 28(9), 1477–1487. Available from: <https://doi.org/10.1002/rra.1538>
- Lassetre, N.S., Piégay, H., Dufour, S. & Rollet, A.-J. (2008) Decadal changes in distribution and frequency of wood in a free meandering river, the Ain River, France. *Earth Surface Processes and Landforms*, 33(7), 1098–1112. Available from: <https://doi.org/10.1002/esp.1605>
- Leckie, D.G., Cloney, E., Jay, C. & Paradine, D. (2005) Automated mapping of stream features with high-resolution multispectral imagery. *Photogrammetric Engineering & Remote Sensing*, 71(2), 145–155. Available from: <https://doi.org/10.14358/PERS.71.2.145>
- Lejot, J., Delacourt, C., Piégay, H., Fournier, T., Trémélo, M.-L. & Allemand, P. (2007) Very high spatial resolution imagery for channel bathymetry and topography from an unmanned mapping controlled platform. *Earth Surface Processes and Landforms: The Journal of the British Geomorphological Research Group*, 32(11), 1705–1725. Available from: <https://doi.org/10.1002/esp.1595>
- Lemaire, P., Piegay, H., MacVicar, B., Mouquet-Noppe, C. & Tougne, L. (2014) Automatically monitoring driftwood in large rivers: preliminary results.
- Lenzi, M.A. (2004) Displacement and transport of marked pebbles, cobbles and boulders during floods in a steep mountain stream. *Hydrological Processes*, 18(10), 1899–1914. Available from: <https://doi.org/10.1002/hyp.1456>
- Lyn, D., Cooper, T. & Yi, Y.-K. (2003) Debris accumulation at bridge crossings: laboratory and field studies. Purdue University: West Lafayette, IN [online] Available from: <https://docs.lib.purdue.edu/jtrp/48> (Accessed 2 March 2020)
- MacVicar, B. & Piégay, H. (2012) Implementation and validation of video monitoring for wood budgeting in a wandering piedmont river, the Ain River (France). *Earth Surface Processes and Landforms*, 37(12), 1272–1289. Available from: <https://doi.org/10.1002/esp.3240>
- MacVicar, B.J., Piégay, H., Henderson, A., Comiti, F., Oberlin, C. & Pecorari, E. (2009) Quantifying the temporal dynamics of wood in large rivers: Field trials of wood surveying, dating, tracking, and monitoring techniques. *Earth Surface Processes and Landforms*, 34(15), 2031–2046. Available from: <https://doi.org/10.1002/esp.1888>
- Marcus, W.A., Legleiter, C.J., Aspinall, R.J., Boardman, J.W. & Crabtree, R. L. (2003) High spatial resolution hyperspectral mapping of in-stream habitats, depths, and woody debris in mountain streams. *Geomorphology*, 55(1–4), 363–380. Available from: [https://doi.org/10.1016/S0169-555X\(03\)00150-8](https://doi.org/10.1016/S0169-555X(03)00150-8)
- Marcus, W.A., Marston, R.A., Colvard, C.R. & Gray, R.D. (2002) Mapping the spatial and temporal distributions of woody debris in streams of the greater Yellowstone ecosystem, USA. *Geomorphology*, 44(3–4), 323–335. Available from: [https://doi.org/10.1016/S0169-555X\(01\)00181-7](https://doi.org/10.1016/S0169-555X(01)00181-7)
- Marcus, W.A., Rasmussen, J. & Fonstad, M.A. (2011) Response of the fluvial wood system to fire and floods in northern Yellowstone. *Annals of the Association of American Geographers*, 101(1), 21–44. Available from: <https://doi.org/10.1080/00045608.2010.539154>
- Mazzorana, B., Ruiz-Villanueva, V., Marchi, L., Cavalli, M., Gems, B., Gschneider, T., Mao, L., Iroumé, A. & Valdebenito, G. (2018) Assessing and mitigating large wood-related hazards in mountain streams: Recent approaches: Assessing and mitigating LW-related hazards in mountain streams. *Journal of Flood Risk Management*, 11(2), 207–222. Available from: <https://doi.org/10.1111/jfr3.12316>
- Montgomery, D.R., Collins, B.D., Buffington, J.M. & Abbe, T.B. (2003) Geomorphic effects of wood in rivers. 21–47 pp.
- Muste, M., Fujita, I. & Hauet, A. (2008) Large-scale particle image velocimetry for measurements in riverine environments. *Water Resources Research*, 44, W00D19.
- Persi, E., Petaccia, G. & Sibilla, S. (2018) Large wood transport modelling by a coupled Eulerian–Lagrangian approach. *Natural Hazards*, 91, 59–74.
- Persi, E., Petaccia, G., Sibilla, S., Brufau, P. & García-Navarro, P. (2019) Calibration of a dynamic Eulerian-lagrangian model for the computation of wood cylinders transport in shallow water flow. *Journal of Hydroinformatics*, 21(1), 164–179. Available from: <https://doi.org/10.2166/hydro.2018.085>
- Petit, S. (2006) Reconstitution de la dynamique du paysage alluvial de trois secteurs fonctionnels de la rivière Allier (1946–2000), Massif Central, France. *Géographie Physique et Quaternaire*, 60(3), 271–287. Available from: <https://doi.org/10.7202/018000ar>
- Piégay, H., Ghaffarian, H., Lemaire, P., Zhang, Z., Boivin, M., Senter, A., Antonio, A., Buffin-Bélanger, T., Lopez, D. & Macvicar, B. (2019) Video-monitoring of wood flux: recent advances and next steps.
- Piégay, H., Gregory, K.J., Bondarev, V., Chin, A., Dahlstrom, N., Elosgi, A., Gregory, S.V., Joshi, V., Mutz, M., Rinaldi, M., Wyzga, B. & Zawiejska, J. (2005) Public perception as a barrier to introducing wood in Rivers for restoration purposes. *Environmental Management*, 36(5), 665–674. Available from: <https://doi.org/10.1007/s00267-004-0092-z>
- Ravazzolo, D., Mao, L., Garniga, B., Picco, L. & Lenzi, M.A. (2013) Displacement length and velocity of tagged logs in the tagliamento river. *Journal of Agricultural Engineering*, 44(2s), 54–57. Available from: <https://doi.org/10.4081/jae.2013.251>
- Ruiz-Villanueva, V., Bladé, E., Sánchez-Juny, M., Martí-Cardona, B., Díez-Herrero, A. & Bodoque, J.M. (2014) Two-dimensional numerical modeling of wood transport. *Journal of Hydroinformatics*, 16(5), 1077–1096. Available from: <https://doi.org/10.2166/hydro.2014.026>
- Ruiz-Villanueva, V., Bodoque, J.M., Díez-Herrero, A., Eguibar, M.A. & Pardo-Igúzquiza, E. (2013) Reconstruction of a flash flood with large wood transport and its influence on hazard patterns in an ungauged mountain basin. *Hydrological Processes*, 27(24), 3424–3437. Available from: <https://doi.org/10.1002/hyp.9433>
- Ruiz-Villanueva, V., Piégay, H., Gurnell, A.M., Marston, R.A. & Stoffel, M. (2016a) Recent advances quantifying the large wood dynamics in river basins: New methods and remaining challenges: Large wood dynamics. *Reviews of Geophysics*, 54(3), 611–652. Available from: <https://doi.org/10.1002/2015RG000514>
- Ruiz-Villanueva, V., Wyzga, B., Mikuš, P., Hajdukiewicz, H. & Stoffel, M. (2016b) The role of flood hydrograph in the

- remobilization of large wood in a wide mountain river. *Journal of Hydrology*, 541, 330–343. Available from: <https://doi.org/10.1016/j.jhydrol.2016.02.060>
- Schmocker, L. & Hager, W.H. (2011) Probability of drift blockage at bridge decks. *Journal of Hydraulic Engineering*, 137(4), 470–479. Available from: [https://doi.org/10.1061/\(ASCE\)HY.1943-7900.0000319](https://doi.org/10.1061/(ASCE)HY.1943-7900.0000319)
- Sendrowski, A. & Wohl, E. (2021) Remote sensing of large wood in high-resolution satellite imagery: Design of an automated classification work-flow for multiple wood deposit types. *Earth Surface Processes and Landforms*, 46(12), 2333–2348. Available from: <https://doi.org/10.1002/esp.5179>
- Senter, A., Pasternack, G., Piégay, H. & Vaughan, M. (2017) Wood export prediction at the watershed scale. *Earth Surface Processes and Landforms*, 42(14), 2377–2392. Available from: <https://doi.org/10.1002/esp.4190>
- Turowski, J.M., Badoux, A., Bunte, K., Rickli, C., Federspiel, N. & Jochner, M. (2013) The mass distribution of coarse particulate organic matter exported from an alpine headwater stream. *Earth Surface Dynamics Discussions*, 1(1), 1–29. Available from: <https://doi.org/10.5194/esurfd-1-1-2013>
- Warren, D.R. & Kraft, C.E. (2008) Dynamics of large wood in an eastern US mountain stream. *Forest Ecology and Management*, 256(4), 808–814. Available from: <https://doi.org/10.1016/j.foreco.2008.05.038>
- Welber, M. (2013) Morphodynamics and driftwood dispersal in braided rivers, PhD Thesis, University of Trento
- Welling, R.T., Wilcox, A.C. & Dixon, J.L. (2021) Large wood and sediment storage in a mixed bedrock-alluvial stream, western Montana, USA. *Geomorphology*, 384, 107703. Available from: <https://doi.org/10.1016/j.geomorph.2021.107703>
- Wilcox, A.C. & Wohl, E.E. (2006) Flow resistance dynamics in step-pool stream channels: 1. Large woody debris and controls on total resistance. *Water Resources Research*, 42(5), 42. Available from: <https://doi.org/10.1029/2005WR004277>
- Wohl, E. (2013) Floodplains and wood. *Earth-Science Reviews*, 123, 194–212. Available from: <https://doi.org/10.1016/j.earscirev.2013.04.009>
- Wohl, E., Angermeier, P.L., Bledsoe, B., Kondolf, G.M., MacDonnell, L., Merritt, D.M., Palmer, M.A., Poff, N.L. & Tarboton, D. (2005) River restoration. *Water Resources Research*, 41(10), W10301. Available from: <https://doi.org/10.1029/2005WR003985>
- Wohl, E., Cenderelli, D.A., Dwire, K.A., Ryan-Burkett, S.E., Young, M.K. & Fausch, K.D. (2010) Large in-stream wood studies: A call for common metrics. *Earth Surface Processes and Landforms*, 35, 618–625. Available from: <https://doi.org/10.1002/esp.1966>
- Wohl, E. & Scott, D.N. (2017) Wood and sediment storage and dynamics in river corridors. *Earth Surface Processes and Landforms*, 42(1), 5–23. Available from: <https://doi.org/10.1002/esp.3909>
- Yin, C., Rosendahl, L., Kær, S.K. & Sørensen, H. (2003) Modelling the motion of cylindrical particles in a nonuniform flow. *Chemical Engineering Science*, 58(15), 3489–3498. Available from: [https://doi.org/10.1016/S0009-2509\(03\)00214-8](https://doi.org/10.1016/S0009-2509(03)00214-8)
- Zhang, Z., Ghaffarian, H., MacVicar, B., Vaudor, L., Antonio, A., Michel, K. & Piégay, H. (2021) Video monitoring of in-channel wood: From flux characterization and prediction to recommendations to equip stations. *Earth Surface Processes and Landforms*, 46(4), 822–836. Available from: <https://doi.org/10.1002/esp.5068>

## SUPPORTING INFORMATION

Additional supporting information can be found online in the Supporting Information section at the end of this article.

**How to cite this article:** Ghaffarian, H., MacVicar, B., Hortobagyi, B., Zhang, Z., Robert, F., Vaudor, L. et al. (2023) Observer-bias and sampling uncertainties in riverine wood flux and volume estimation from video monitoring technique. *Earth Surface Processes and Landforms*, 48(3), 525–536. Available from: <https://doi.org/10.1002/esp.5500>